

# Unscented Kalman Filter for Vision based Target Localisation with a Quadrotor

Jos Alejandro Dena Ruiz and Nabil Aouf

*Centre of Electronic Warfare, Defence Academy of the United Kingdom,  
Cranfield University, Shrivenham, SN6 8LA, U.K.*

**Keywords:** UAV, Unscented Kalman Filter, Optitrack, ROS.

**Abstract:** Unmanned aerial vehicles (UAV) equipped with a navigation system and an embedded camera can be used to estimate the position of a desired target. The relative position of the UAV along with knowledge of camera orientation and imagery data can be used to produce bearing measurements that allow estimation of target position. The filter methods applied are prone to biases due to noisy measurements. Further noise may be encountered depending on the UAV trajectory for target localisation. This work presents the implementation of an Unscented Kalman Filter (UKF) to estimate the position of a target on the 3D cartesian plane within a small indoor scenario. A small UAV with a single board computer, equipped with a frontal camera and moving in an oval trajectory at a fixed height was employed. Such a trajectory enabled an experimental comparison of UAV simulation data with UAV real-time flight data for indoor conditions. Optitrack Motion system and the Robot Operative System (ROS) were used to retrieve the drone position and exchange information at high rates.

## 1 INTRODUCTION

Unmanned Aerial Vehicles (UAV) have proven to be a reliable platforms for research. The quadrotor UAV has been one of the most popular among the different UAV types, due to the easy architecture and its capabilities in reaching areas where no other UAV can. The small size and the vertical take-off and landing are two of the main advantages this UAV offers.

This paper presents the use of a small quadrotor with an onboard embedded camera for target localisation on indoor conditions at low height. Visual measurements of the target based on the pixel position on the image can be transformed into two bearing measurements, dependent upon the vehicle position and orientation (Ponda, 2008). The use of bearing angles based only on the pixel position is not enough to determine the target localisation without the range (and with noisy measurements), therefore an Unscented Kalman Filter (UKF) is implemented to estimate a stationary target position within the 3D plane. The estimation results are influenced by the drone's trajectory. Therefore an oval trajectory was chosen in order to vary both measured angles within a small area.

Several pieces of research have been done related to target localisation with UAV, like the use of fixed

wing vehicles with visible cameras on (Hosseinpoor et al., 2016); (Wang et al., 2016). (Ponda, 2008) presented the use of an Extended Kalman Filter for target localisation with a fixed-wing drone and a gimballed camera, showing simulation results of a localised object being orbited by the drone at 100 ft height and with an orbit of 50 ft radius, achieving the final estimated values after 100 measurements. Similarly, (Redding et al., 2008) used a Recursive Least Squares (RLS) filter to estimate the target position, achieving experimental results using a fixed-wing miniature drone with a circular orbit of 50 m radius and 60 m altitude, obtaining an estimation with an error of 10.9 m after 20 seconds of trajectory. (Deneault et al., 2008) presented the tracking for ground targets using an Unscented Transformation. To obtain the required measurements, mean and covariance data for the target position as a function of the SLAM states and camera measurements were used. (Hou and Yu, 2014) show the use of a Pelican quadrotor for target localisation, using a configuration of a frontal camera, ultrasonic and laser sensors. The use of these three devices determined the current drone position. An onboard visible camera was used for object colour detection, experiments shows the target localisation using this setup. (Jung et al., 2016) presented the use

of an UKF to estimate the position of a moving target with three different process model. Simulations on Matlab show different estimation error for each model where a camera pointing downwards is tracking the moving target for landing purposes. (Gomez-Balderas et al., 2013) used a quadrotor for target localisation and tracking, controlling the UAV based on the target localisation to keep it on the field of view, all under indoor conditions.

## 2 TECHNICAL APPROACH

A simple projection of the target on the image is presented in Figure 1. Where the camera pointing axis is well known, the UAV position is obtained by a motion capture system and the orientation by the onboard Inertial Measurement Unit (IMU). This way the pixel location can be transformed into two bearing angles ( $\alpha_1$  and  $\alpha_2$ ) from the camera pointing axis to a vector that passes through the target and the camera focal point. Using a series of rotations from the camera frame to the UAV body frame, and from the body frame to the earth frame, these angles can be converted into overall azimuth and elevation angles ( $\beta$  and  $\phi$ ), Figure 2, which define the bearing angles between the UAV and the target.

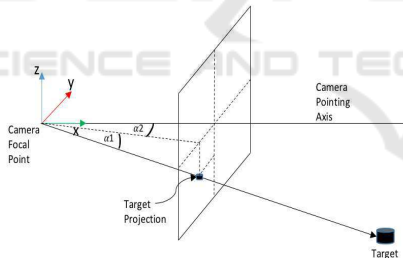


Figure 1: Image measurement projection based on the target pixel position.

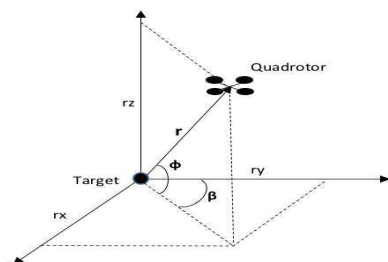


Figure 2: Azimuth and Elevation  $\beta$  and  $\phi$ .

## 3 PLATFORM VEHICLE AND SCENARIO

A Pelican quadrotor from Ascending Technologies (AscTec) was chosen as the prototype to develop the experiments, as its physical architecture made of carbon fibre and both well distributed sensors and components make it a reliable platform for research purposes. This quadrotor offers plenty of space and various interfaces for individual components and payloads. Figure 3.

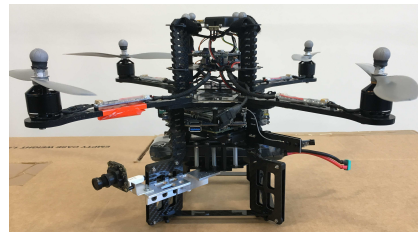


Figure 3: Quadrotor AscTec Pelican used to develop the experiments.

The basic electronic components are the AscTec Autopilot, motor controllers and a single board computer named the Mastermind. The AscTec Autopilot also known as Flight-Control-Unit(FCU), contains the High Level Processor and the Low Level Processor (LLP and HLP) running at 1 kHz, which are in charge of aircraft control. The LLP handles sensor data processing and data fusion, as well as a stable attitude control algorithm. The HLP is open for the user purposes, like the implementation of control algorithms, sensor fusion, etc.

The AscTec Mastermind is an onboard processor board, its weight of 400 grams and size 10X10X5 cm offers an extremely high processing power, high data rates and a great variety of standard PC interfaces. Features like a Dual Core Atom, a Core 2 Duo, or a Core i7, WIFI, Firewire and hardware serial ports are supported. Running Ubuntu 14.04 as operative system, the user has plenty of programming possibilities.

The Optitrack Motion Capture System, was used to retrieve the ground truth position. The full setup to get the ground truth is composed of six cameras connected to a 12-port POE switch, along with a host computer with Optitrack Motive application, that runs and streams the current position of the rigid body at 120 Hz. The position is published on ROS and retrieved by the Mastermind which is also connected to the same wireless network, Figure 4.

The platform was also equipped with an mvBlueFox-IGC visible camera, the images are obtained through a ROS package at 20 Hz and published into the ROS network for its future processing.

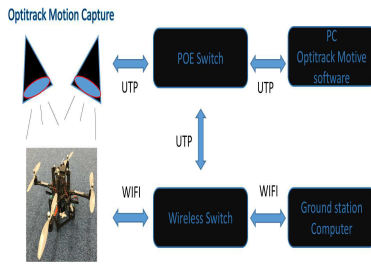


Figure 4: Quadrotor Control System overview.

## 4 VISION-BASED TARGET LOCALISATION

This section describes the problem of target localisation using vision-only. The measurements are obtained from the camera on the quadrotor. For the purpose of this project, the image processing for target recognition is assumed and the pixel location corresponding to the centre of the target is available. This way, the images from the image sensors can be converted into bearings-only measurements, which can be processed using the UKF to estimate the location of the target. Considering that the target is stationary, the estimation time and accuracy will be highly influenced by the drone's path. In this case an oval with radius of  $r1 = 1$  m (in the short axis) and radius  $r2 = 1.5$  m (in the long axis) and a constant height of 0.5 m were chosen in order to vary the measurements as much as possible in a reduced area.

The target dynamics model is assumed to be linear but the measurement model is still non-linear, giving the following system dynamics,

$$X_{k+1} = \Phi_{k+1,k} X_k + W_k \quad (1)$$

$$Z_k = h(X_k) + V_k \quad (2)$$

where  $\Phi_{k+1,k}$  is the state transition matrix of the system from the time  $k$  to  $k+1$  and  $W_k$  and  $V_k$  are the process and measurement noise, which are uncorrelated, Gaussian and white with zero mean and covariance  $Q_k$  and  $R_k$  respectively.

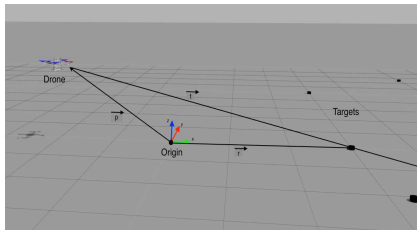


Figure 5: Target and vehicle vector representation

The measurement model involves two bearing measurements and is given by

$$h_{x_k} = \begin{bmatrix} \beta \\ \phi \end{bmatrix} = \begin{bmatrix} \tan^{-1}(\frac{r_x}{r_y}) \\ \tan^{-1}(\frac{r_z}{\sqrt{(r_x)^2 + (r_y)^2}}) \end{bmatrix} \quad (3)$$

where  $r_x = p_x - t_x$ ,  $r_y = p_y - t_y$ ,  $r_z = p_z - t_z$ .

$p_k = [p_x \ p_y \ p_z]^T$  is the quadrotor position,  $t_k = [t_x \ t_y \ t_z]^T$  is the target estimated position and  $r_k = [r_x \ r_y \ r_z]^T$  the relative vector between the vehicle and the target respectively, Figure 5.

## 5 UNSCENTED KALMAN FILTER

The UKF algorithm is composed by the time update and measurement update steps. The time update includes the weights and sigma points calculations, whereas the measurement update uses the sigma points to generate the covariance matrices and the kalman gain respectively.

### 5.1 Time Update

First, weights are defined as:

$$W_1 = \frac{\lambda}{n + \lambda} \quad (4)$$

$$W_i = \frac{1}{2(n + \lambda)} \quad i = 1, 2, \dots, n \quad (5)$$

where  $n$  is the dimension of the state vector and  $\lambda$  is an arbitrary constant. The sigma points at time step  $k$  calculate as:

$$S_{k-1} = chol((n + \lambda)P_{k-1}) \quad (6)$$

$$X_{(0)} = \hat{x}_{k-1} \quad (7)$$

$$X_{(i)} = \hat{x}_{k-1} + S_{k-1}^{(i)} \quad i = 1, 2, \dots, n \quad (8)$$

$$X_{(i+n)} = \hat{x}_{k-1} - S_{k-1}^{(i)} \quad i = 1, 2, \dots, n \quad (9)$$

$$X_{k-1} = [X_{(0)} \ X_{(1)} \ \dots \ X_{(2n)}] \quad (10)$$

$chol$  means cholesky decomposition and  $S^{(i)}$  mean  $i$ th row vector of  $S$ . The time update equations are:

$$\hat{X}_k = \sum_{i=0}^{2n} W_i f(X_i) \quad (11)$$

$$P_k = \sum_{i=0}^{2n} W_i \{f(X_i) - \hat{X}_k\} \{f(X_i) - \hat{X}_k\}^T + Q_k \quad (12)$$

## 5.2 Measurement Update

The augmented sigma points are calculated as follows:

$$S_k^- = chol((n + \lambda)P_k^-) \quad (13)$$

$$X_{(0)}^- = \hat{x}_k^- \quad (14)$$

$$X_{(i)}^- = \hat{x}_k^- + S_k^{(i)} \quad i = 1, 2, \dots, n \quad (15)$$

$$X_{(i+n)}^- = \hat{x}_k^- - S_k^{(i)} \quad i = 1, 2, \dots, n \quad (16)$$

$$X_k^- = [X_{(0)}^- \quad X_{(1)}^- \cdots X_{(2n)}^-] \quad (17)$$

$$\hat{z}_k^- = \sum_{i=0}^{2n} W_i h(X_i) \quad (18)$$

The measurement update equations are:

$$P_z = \sum_{i=0}^{2n} W_i \{h(X_i) - \hat{z}_k^-\} \{h(X_i) - \hat{z}_k^-\}^T + R \quad (19)$$

$$P_{xz} = \sum_{i=0}^{2n} W_i \{f(X_i) - \hat{x}_k^-\} \{h(X_i) - \hat{z}_k^-\}^T \quad (20)$$

The Kalman gain is calculated as:

$$K_k = P_{xz} P_z^{-1} \quad (21)$$

Finally, the estimated states and its covariance matrix are:

$$\hat{X}_k = \hat{X}_k^- + K_k (z_k - \hat{z}_k^-) \quad (22)$$

$$P_k = P_k^- - K_k P_z K_k^T \quad (23)$$

For this scenario with a stationary target, the process noise is zero because the target position is constant. The process model, process error covariance matrix and the measurement covariance error are:

$$\Phi_{k,k-1} = \begin{bmatrix} 1 & 0 & 0 \\ 0 & 1 & 0 \\ 0 & 0 & 1 \end{bmatrix}, Q_k = \begin{bmatrix} 0 & 0 & 0 \\ 0 & 0 & 0 \\ 0 & 0 & 0 \end{bmatrix} \quad (24)$$

$$R_k = \begin{bmatrix} \sigma_1^2 & 0 \\ 0 & \sigma_2^2 \end{bmatrix} \quad (25)$$

## 6 SIMULATION AND EXPERIMENTAL RESULTS

The target estimation algorithm for simulations and experiments was initialised with the following parameters,

$$\hat{X}_0 = \begin{bmatrix} 20 \\ 20 \\ 20 \end{bmatrix}, P_0 = \begin{bmatrix} 50 & 0 & 0 \\ 0 & 50 & 0 \\ 0 & 0 & 50 \end{bmatrix}, \lambda = 0 \quad (26)$$

in both cases, the quadrotor trajectory is running at 15Hz (step  $k=0.066$  sec) and 0.01 radians per step. At every step the camera takes an image which is processed to locate the target. Once the pixel that represents the centre of the target is obtained this pixel is mapped into the bearing angles, which will be taken by the UKF along with the drone position and orientation, to estimate the 3D target position.

### 6.1 Simulation

Gazebo Simulator and ROS were used as the virtual environment to simulate the estimation, the package *rotors\_simulator* (Furrer et al., 2016) provides some multi-rotor models such as the AscTec Hummingbird, the AscTec Pelican, or the AscTec Firefly. In the package files, the user can select the model to work with as well as plenty of sensors. The Pelican quadrotor and a visible camera were selected. A small black cylinder was used as a target for simulations (Figure 6), positioned on the 3D plane coordinates 2.85, 0.05 and 0.0 (x, y, z respectively). For this simulation, the noise that affects the measurement is coming from the camera. White gaussian noise with zero mean noise was added with standard deviation  $\sigma = 0.007$ . Figure 7 shows the target position and UAV trajectory, whereas Figures 9-11 show the estimated results for each axis.



Figure 6: Image retrieved from the virtual image sensor pointing at the target.

### 6.2 Experiments

The experiments were performed in indoor conditions. To control the Pelican quadrotor position, Optitrack Motion Capture was used to feedback the ground truth, which is published by ROS at 120 Hz. As a target on the real UAV flight experiments a red cup was used for simplicity, positioned in the same coordinates as on simulations (Figure 11). The image sensor used for the experiment was the BlueFox IGC202C, publishing images at 20 Hz on ROS. The

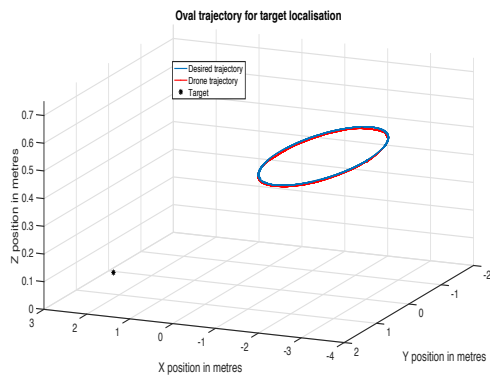


Figure 7: 3D view of the flight path on simulations and target position.

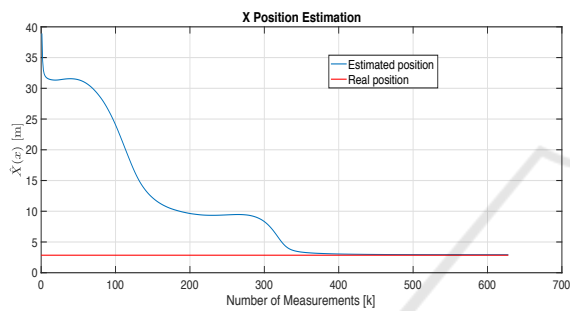


Figure 8: Estimation of  $\hat{X}(x)$  on simulation.

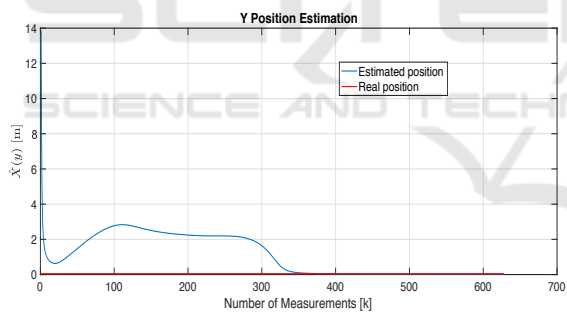


Figure 9: Estimation of  $\hat{X}(y)$  on simulation.

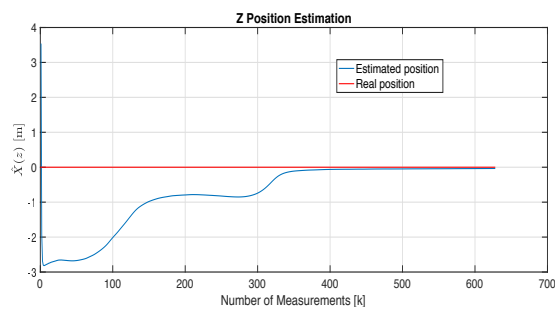


Figure 10: Estimation of  $\hat{X}(z)$  on simulation.

use of gimbal was not necessary, because the target never left the camera field of view. The noise on the measurement is coming from the image sensor.

Several tests with the target and Drone being stationary were made in order to get the variance of this noise,  $\sigma_1^2 = 4.65 \times 10^{-5}$  and  $\sigma_2^2 = 6.5 \times 10^{-8}$ . Figure 12 shows the target position and UAV trajectory, Figure 13 shows the noisy measurements and Figures 14-16 show the estimated results for each axis.

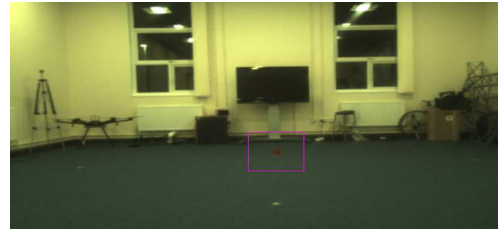


Figure 11: Image retrieved from the image sensor on experiments.

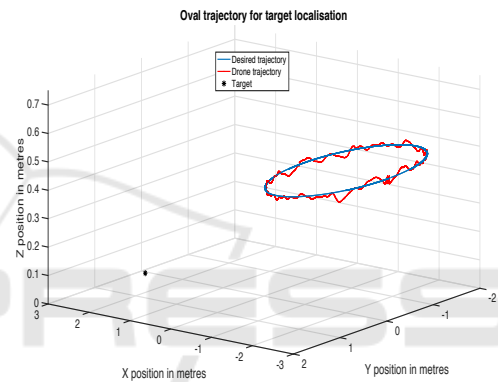


Figure 12: 3D view of the flight path on experiments and target position.

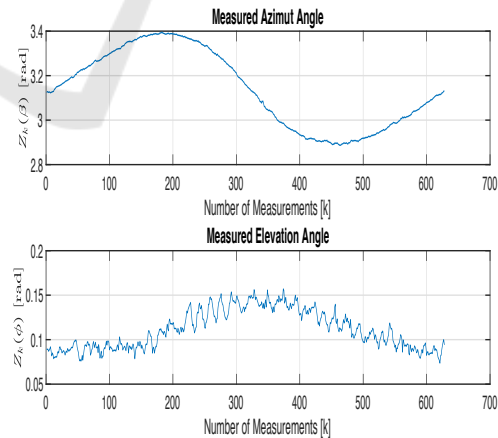


Figure 13: Measurements ( $Z_k$ ), Azimut ( $\beta$ ) and Elevation ( $\phi$ ) angles based on the pixel position.

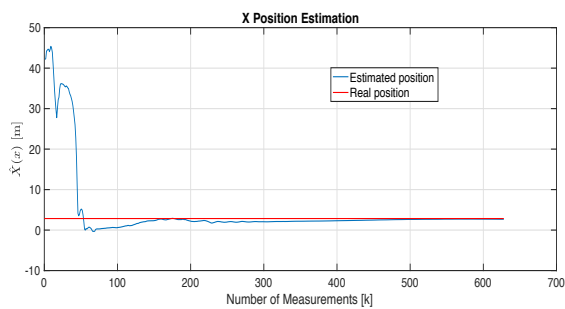


Figure 14: Estimation of  $\hat{X}(x)$  on experiment.

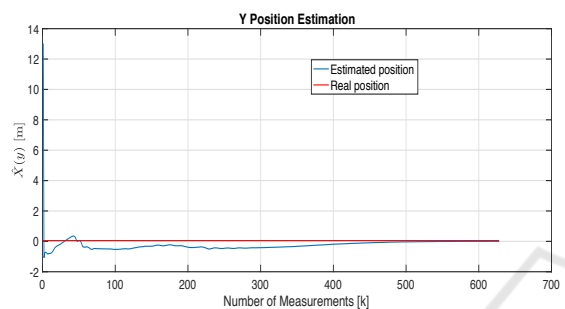


Figure 15: Estimation of  $\hat{X}(y)$  on experiment.

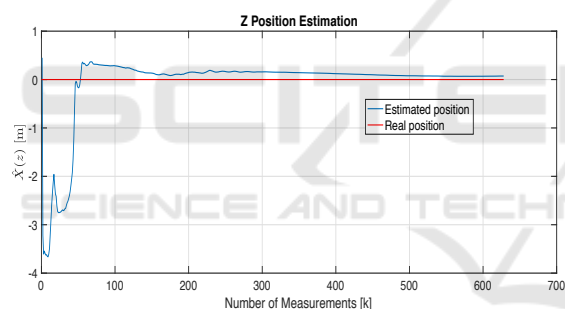


Figure 16: Estimation of  $\hat{X}(z)$  on experiment.

## 7 CONCLUSIONS

This paper shows the implementation of an UKF for target localisation with simulations and experimental results using bearing angles only. The quadrotor uses a frontal camera that captures the target on the image. The image is processed in order to obtain the pixel that represents the target centre, which along with the drone position and orientation, can be converted into the azimuth and elevation. The UKF was fed with the noisy azimuth and elevation angles and estimates the 3D target position. The simulation results show that the estimated values converged into the real values after 400 measurements on the 3 axis, whereas in the experimental results the estimated values converged in 500 measurements. On real and simulation results, the  $\hat{X}(z)$  axis presents the bigger error in steady state 0.07 m and 0.035 m, due to the lack

of the vector range between the drone and the target. The final errors for  $\hat{X}(x)$  and  $\hat{X}(y)$  on simulation were 0.07 m and 0.028 m, as opposed to 0.018 m and 0.05 m for experimental results. The simulation was ran under Gazebo Simulator and ROS, whereas for UAV real-time flight experiments Optitrack and ROS were used to perform the full estimation algorithm. The complete set-up allowed us to perform the estimation in real-time, and achieving the target position after 30 seconds of trajectory. The use of additional, different trajectories would reduce the estimation time like showed (Ponda, 2008), although for indoor environments with a reduced area, the presented trajectory and estimator performed successfully.

## REFERENCES

- Deneault, D., Schinstock, D., and Lewis, C. (2008). Tracking ground targets with measurements obtained from a single monocular camera mounted on an unmanned aerial vehicle. *Proceedings - IEEE International Conference on Robotics and Automation*, pages 65–72.
- Furrer, F., Burri, M., Achtelik, M., and Siegwart, R. (2016). RotorSA modular gazebo MAV simulator framework. *Studies in Computational Intelligence*, 625:595–625.
- Gomez-Balderas, J. E., Flores, G., García Carrillo, L. R., and Lozano, R. (2013). Tracking a Ground Moving Target with a Quadrotor Using Switching Control. *Journal of Intelligent & Robotic Systems*, 70(1-4):65–78.
- Hosseinpoor, H. R., Samadzadegan, F., and Dadrasjavan, F. (2016). Precise Target Geolocation and Tracking Based on Uav Video Imagery. In *ISPRS - International Archives of the Photogrammetry, Remote Sensing and Spatial Information Sciences*, volume XLI-B6, pages 243–249.
- Hou, Y. and Yu, C. (2014). Autonomous target localization using quadrotor. *26th Chinese Control and Decision Conference, CCDC 2014*, pages 864–869.
- Jung, W., Kim, Y., and Bang, H. (2016). Target state estimation for vision-based landing on a moving ground target. *2016 International Conference on Unmanned Aircraft Systems, ICUAS 2016*, pages 657–663.
- Ponda, S. (2008). Trajectory Optimization for Target Localization Using Small Unmanned Aerial Vehicles. *AIAA Guidance, Navigation, and Control Conference*, (August).
- Redding, J., McLain, T., Beard, R., and Taylor, C. (2008). Vision-based Target Localization from a Fixed-wing Miniature Air Vehicle. *2006 American Control Conference*, 44(4):2862–2867.
- Wang, X., Liu, J., and Zhou, Q. (2016). Real-time multi-target localization from Unmanned Aerial Vehicle. *Sensors*, pages 1–19.